Chapter 2

Rapid Solidification of Undercooled Melts

Xiaolong Xu, Hua Hou and Feng Liu

Additional information is available at the end of the chapter

http://dx.doi.org/10.5772/intechopen.70666

Abstract

Rapid solidification and microstructure evolution of deeply undercooled bulk concentrated Ni-20%at.Cu and Co-20%at.Pd alloys are strictly and systematically evaluated. First, thermodynamics of the undercooled melt is discussed. Consideration is provided for not only the systematic microstructure evolution within a broad undercooling range, but also the dendrite growth mechanism and the rapid solidification characteristics. The dendrite growth in the bulk undercooled melts was captured by a high speed camera. The first kind of grain refinement occurring in the low undercooling regimes was explained by a current grain refinement model. Besides for the dendrite melting mechanism, the stress originating from the solidification contraction and thermal strain in the first mushy zone during rapid solidification could be a main mechanism causing the second kind of grain refinement above the critical undercooling. This internal-stress led to the distortion and breakup of the primary dendrites and was semi-quantitatively described by a corrected stress accumulation model. It was found that the stress induced recrystallization could make the primary microstructures refine substantially after recalescence.

Keywords: rapid solidification, undercooling, grain refinement, alloys, stress, recrystallization

1. Introduction

Grain refinement is an interesting phenomenon that has an important scientific significance and has been numerously investigated [1–22]. In order to understand of grain refinement phenomenon better, numerous studies have been extensively executed and many different grain refinement mechanisms were suggested separately, such as dynamic nucleation [1], critical growth velocity [5, 6], kinetics induced growth instabilities [2–4], dendrite fragmentation [7, 9], dendrite remelting and [8, 9] recrystallization [7]. In 1959, Walker [1–8] had been firstly investigated the grain refinement event occurring in the rapid solidification of deeply undercooled pure Nickel melt. He found that the grain size would abruptly refine when the

initial undercooling ΔT prior to nucleation exceeded a critical value. Thereafter, Powell [5] also found the existence of a critical undercooling when he investigated the microstructural evolution of Ag, Cu and Ni based alloys as a function of undercooling. Powell suggested that the recrystallization process during recalescence and post-recalescence periods would be responsible for the grain refinement at high undercooling ranges [5]. Herlach [6] measured the dendrite growth velocity in many undercooled melts, and he found that critical undercooling was correlated to a critical crystal growth velocity, which was about 20 m/s and was the solute diffusion velocity V_D in the undercooled melts. In the recent years, grain refinement occurring at undercoolings much lower than ΔT^* has attracted much attention [10–12]. During the post-recalescence period, the uniformly massive dendrite breakup will occur though the dendrite remelting. Karma [8] has proposed a physical mechanism which suggests that the break-up of dendrites due to remelting brings about the grain refinement both at low and high undercooling regimes. However, this model only considered the remelting due to liquid/solid interface tension, ignoring the effect of the chemical superheating [9] during recalescence, which may also play a much more important role in the dendrite remelting, and has a stronger influence on the final grain morphology. It is the main subject of the present paper to extend the current chemical superheating model to non-equilibrium solidification conditions and fully explain the dendrite remelting mechanism of the grain refinement events.

In the present study, we choose Ni-20at.%Cu alloy and Co-20at.%Pd alloy. The authors experimentally investigated the microstructural evolution of the Ni-20at.%Cu alloys as a function of initial undercooling and the physical mechanisms of the grain refinements occurring at low undercooling regimes. In combination with the current dendrite growth model, we theoretically analyzed the dendrite remelting in the undercooled alloys by an extended chemical superheating model for non-equilibrium solidification of undercooled binary single phase alloys.

2. Material and methods

Ni-20at.%Cu (atomic percent) alloy and Co-20at.%Pd (atomic percent) alloy samples each weighing about 3 g, were prepared by *in situ* melting pure Ni pieces (99.95% purity) and pure Cu pieces (99.9 wt.% purity), pure Co pieces (99.99% purity) and pure Pd pieces (99.99 wt.% purity), under the protection of argon (Ar) atmosphere in a vacuum chamber. Before melting, the surfaces of the metals were cleaned and grinded off mechanically to remove the surface oxide layer and were etched chemically in HCl solution diluted by alcohol. A high purity quartz crucible containing the alloy specimen was placed in the center of an induction coil. The melting process was conducted in the vacuum chamber. Undercooling experiment was executed by using of fluxing liquid and high frequency induction heating and thermal cycle under the protection of argon atmosphere. The vacuum chamber was evacuated and subsequently backfilled with 99.99% argon gas. Each sample was melted, superheated, solidified and subsequently remelted in superheating–cooling cycles to obtain various undercoolings. For each of the alloys, 20–30 undercoolings were made and a natural cooling rate of 20 K/s IS applied in these experiments. After the high frequency power source was turned off, the alloy sample

was spontaneously cooled to room temperature, while the cooling curve of the specimen was monitored by an infrared pyrometer with an accuracy of 5 K and a response time of 10 ms.

3. Solidification process

In the present study, we used a high speed camera to capture the solidification process, i.e., to capture the heat releasing process upon solidification. It can be seen from **Figure 1** that for ΔT = 95 K (95°C), 160 K (160°C), 200 K (200°C) and 270 K (270°C), the nucleation of the undercooled melts all started from the interface between the B_2O_3 glass and the undercooled melt. However, for a higher enough undercooling, ΔT = 320 K (320°C), the start stage of heat releasing process was between the walls of the quartz crucible and the undercooled melts. It is generally considered that the higher of the extent of purification of an undercooled melt, the higher undercooling could be achieved. In addition, the impurities are mainly in the B_2O_3 melt and the interface between B_2O_3 melt and the undercooled melt. The present experiment phenomenon proves that the instabilities of the undercooled melts (i.e., nucleation) with ΔT = 95 K (95°C), 160 K (160°C), 200 K (200°C) and 270 K (270°C) are mainly due to the impurities absorbed in the interface between the B_2O_3 melt and the undercooled melt. However, for the higher undercooled alloy ΔT = 320 K (320°C), the impurities are rather less and the instabilities of the undercooled melt was in the interface between the quartz crucible and the

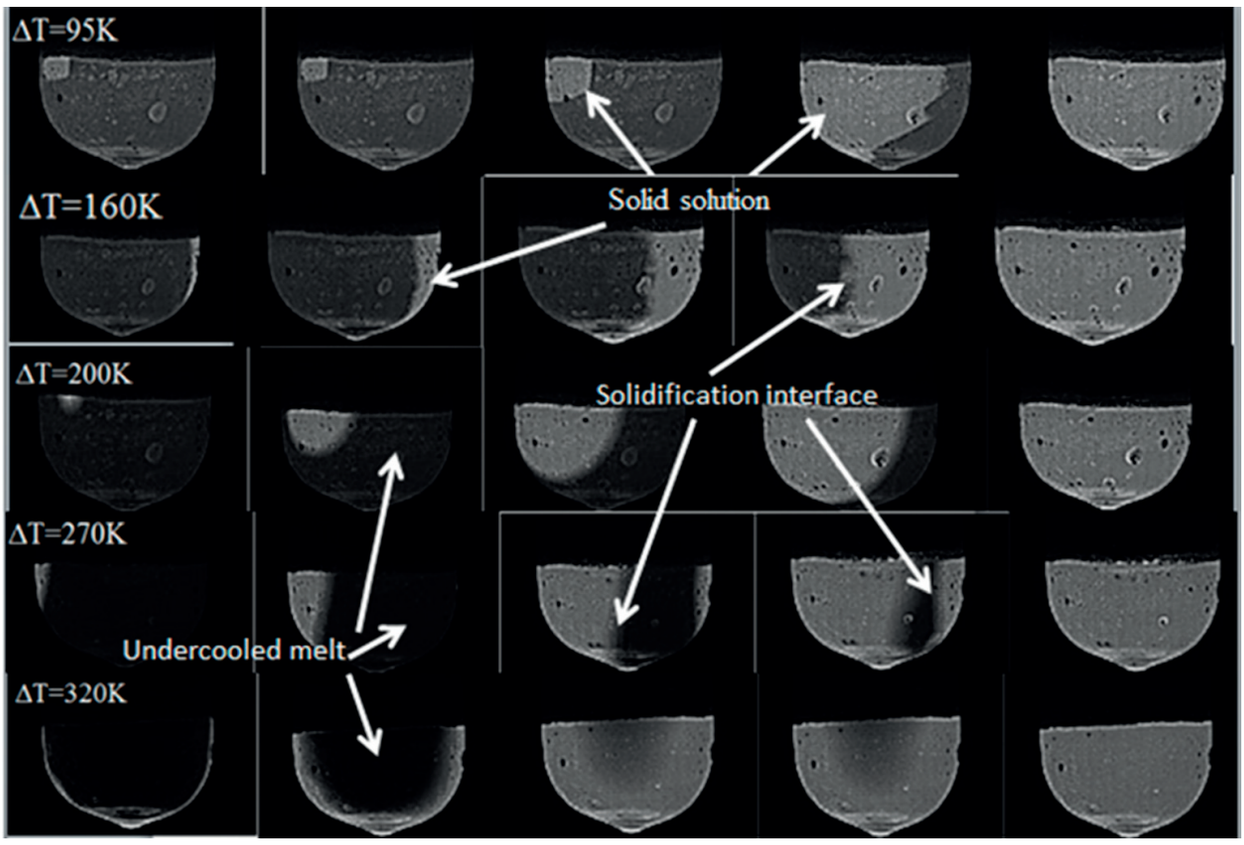

Figure 1. The high-speed video pictures of the undercooled Ni-20at.%Cu different undercoolings.

undercooled melt. Besides, it can be seen that multiple nucleation of solidification occurred. During rapid solidification of the undercooled melts, such as 95 K (95°C) and 160 K (160°C), it can be seen that the coarse primary dendrites are growing towards the undercooled residual melt. However, at high undercoolings such as 200 K (200°C), 270 K (270°C) and 320 K (320°C), much finer dendrites are growing into the melts. Thus, it can be concluded that the higher the undercooling of the melt, the finer the growing dendrites would be.

4. Dendrite growth analysis

Firstly, we need to use the BCT model by Boettinger, Coriell and Trividi [13] to calculate the solidification parameters. According to the models, the initial undercooling ΔT at the dendrite tip consists of four parts,

$$\Delta T = \Delta T_r + \Delta T_c + \Delta T_k + \Delta T_t \tag{1}$$

where ΔT_r, ΔT_k, ΔT_c, and ΔT_t are the thermal undercooling, solutal undercooling, curvature undercooling and interfacial kinetic undercooling, respectively. Details of the BCT model are referred to Ref. [13].

Using the physical parameters of the Ni-20at.%Cu alloy listed in **Table 1**, the undercooling components, the crystal growth velocity and the tip radius at the growing dendrite tip, can be calculated. The results are illustrated in **Figures 2** and **3**. It should be clarified that the table is original and we are using only data from Ref. [11].

It is well known that [13–15], in a single phase alloy, the condition of diffusional equilibrium is gradually becoming less important with the increase of solidification velocity and undercooling in front of the dendrite tip. Therefore, solute rejection is reduced and solutal undercooling decreases as the interface concentration approaches the melt composition. This ultimately causes partitionless solidification, which is solely controlled by thermal gradient. For Ni-20at.%Cu alloys (**Figure 2**), when the initial undercooling ΔT < 35 K (35°C), the solute undercooling ΔT_c is larger than those of other undercooling components, so the dendrite growth in the undercooled melt is mainly controlled by the solute diffusion in front of the dendrite tip and the crystal growth velocity is very low, therefore, coarse dendrites can be resultant. As the undercooling continuously increases, the effect of thermal diffusion on the dendrite growth becomes strong. In the undercooling range of about 35 K (35°C) < ΔT < 65 K (65°C), ΔT_t starts to exceed ΔT_c, which reaches a maximum at ΔT = 55 K (55°C) where the dendrite tip also reaches its maximum and is the most unstable due to the maximum solute undercooling. In this undercooling range, the action of solute undercooling ΔT_c and thermal undercooling ΔT_t is on the same level. When ΔT > 70 K (70°C), ΔT_t increases rapidly and exceeds ΔT_c substantially, the dendrite tip radius accordingly decreases (**Figure 3**) and the crystal growth rate V increases rapidly (**Figure 3**). The increasing action of thermal diffusion results in directionality of dendrites. Solute diffusion is replaced by the thermal diffusion to predominantly control the dendrite growth process, which indicates a transition from the equilibrium of a solidification controlled by the solutal gradient to a thermally controlled growth process owing to a relaxation of diffusional equilibrium at the

http://dx.doi.org/10.5772/intechopen.70666

Parameters	Value of Ni-20at.%Cu alloys
Heat of fusion ΔH_f/kJ mol^{-1}	17,160
Specific heat of the liquid C_p/J^{-1} mol^{-1} K^{-1}	38.5
Dynamic viscosity of the liquid μ/Pas	10^{-3}
Molar volume of the liquid V_m^L/m^3 mol^{-1}	8.06×10^{-6}
Molar volume of the solid V_m^S/m^3 mol^{-1}	7.08×10^{-6}
Liquidus T_L/K	1680 K (1407°C)
Solute diffusivity in the liquid D_L/m^2 s^{-1}	3×10^{-9}
Thermal diffusivity α_L/m^2 s^{-1}	7×10^{-6}
Atomic space a_0/m	4×10^{-10}
Interfacial energy $\sigma_{S,L}$/J m^{-2}	0.29
Speed of sound in the melt V_0/m s^{-1}	4000
Equilibrium liquidus slope m_L/K (at%)$^{-1}$	−2.525
Equilibrium solute partition coefficient k_0	0.724
Solidification time t_f/s	0.1
Size of the mushy zone a/m	0.01
Gibbs–Thomson coefficient Γ	3.25×10^{-7}
Solid fraction at the dendrite coherency point f_S^{coh}	0.15
Solidification shrinkage of the primary phase β	0.1215
Atomic diffusive speed V_D/m s^{-1}	20

Table 1. Physical parameters used in the calculation [9].

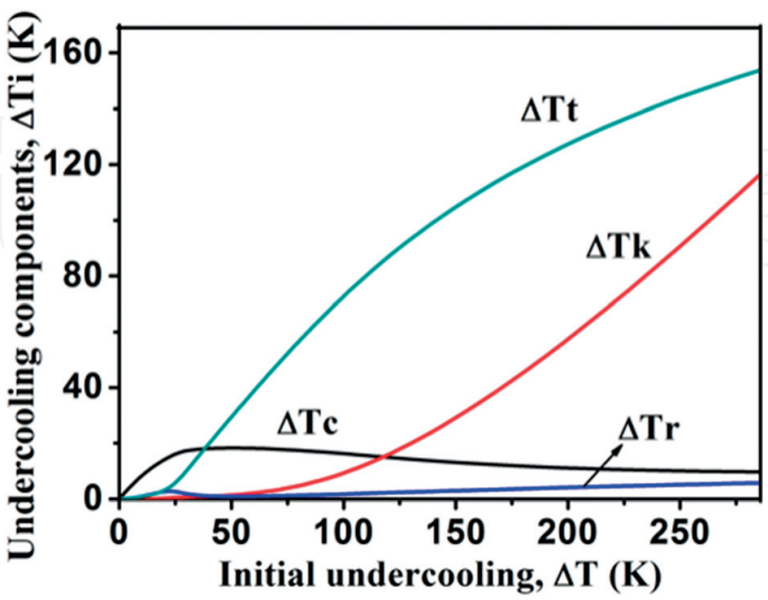

Figure 2. The undercooling constituents as a function of initial undercoolings for Ni-20at.%Cu alloys.

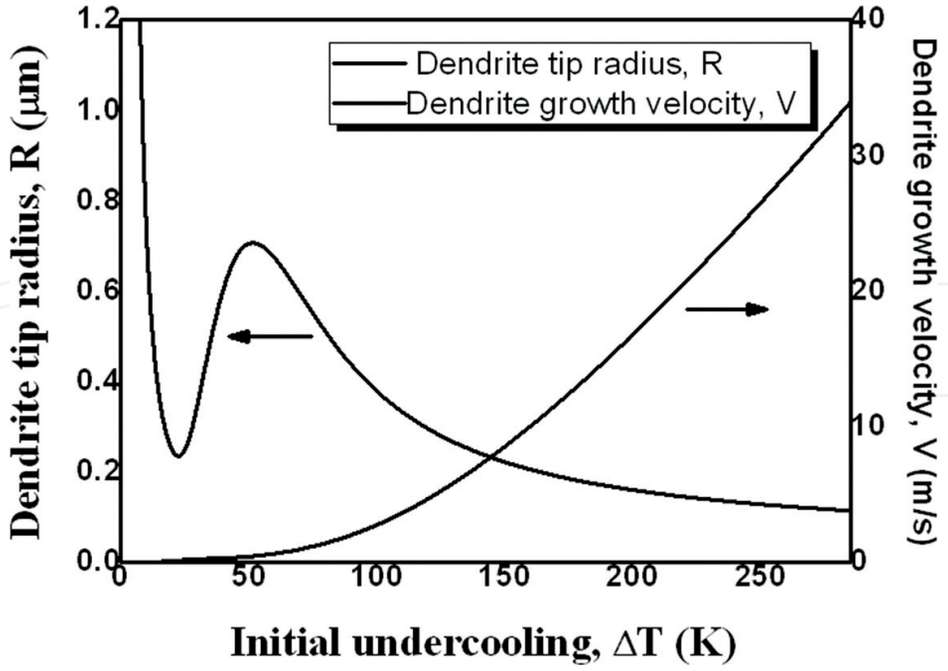

Figure 3. The variation of dendrite tip radius and growth velocity as a function of initial undercoolings for Ni-20at.%Cu alloys.

solid/liquid interface. Therefore, the higher the initial undercooling and the thermal undercooling, the more convenient it becomes for dissipating of the latent heat at the dendrite tip during the crystal growth.

5. Structure evolution of undercooled alloys

As the increasing of undercooling, the Ni-20%at.Cu alloys undergo two kinds of grain refinements: one taking place at low undercoolings, and the other occurring at high undercoolings. The grain sizes and the corresponding typical microstructures at various undercoolings are shown in **Figure 4**. Pioneer investigations [1–11] have shown that as the initial undercooling increases, the microstructures of the deeply undercooled binary single phase solid solution alloys evolves as: coarse dendrites → fine equiaxed grains →coarse dendrites plus fine equiaxed grains → fine equiaxed grains. In the present investigation, we found that the microstructural evolution of the deeply undercooled Ni-20%at.Cu alloys was basically follows the above law. Subjected to small undercoolings, e.g., at $\Delta T < \Delta T_1 = 45$ K, the solidification microstructures were coarse dendrites (**Figure 4a** and **b**) with highly developed secondary dendritic arms. As increasing ΔT, coarse dendrites gradually refined into granular grains by remelting. For the samples nucleated at undercooling about $\Delta T_1 - \Delta T_2 = 90$ K, the overall solidification microstructures are occupied by fine grains (**Figure 4c**) with a few dendrite skeletons, as shown in the black ellipse marked in **Figure 4c**. A further increase of the undercooling leads to the rising of the grain size again. When $\Delta T > \Delta T_3 = 110$ K, much finer dendrite beams form because of that the controlling mechanism of dendrite

http://dx.doi.org/10.5772/intechopen.70666

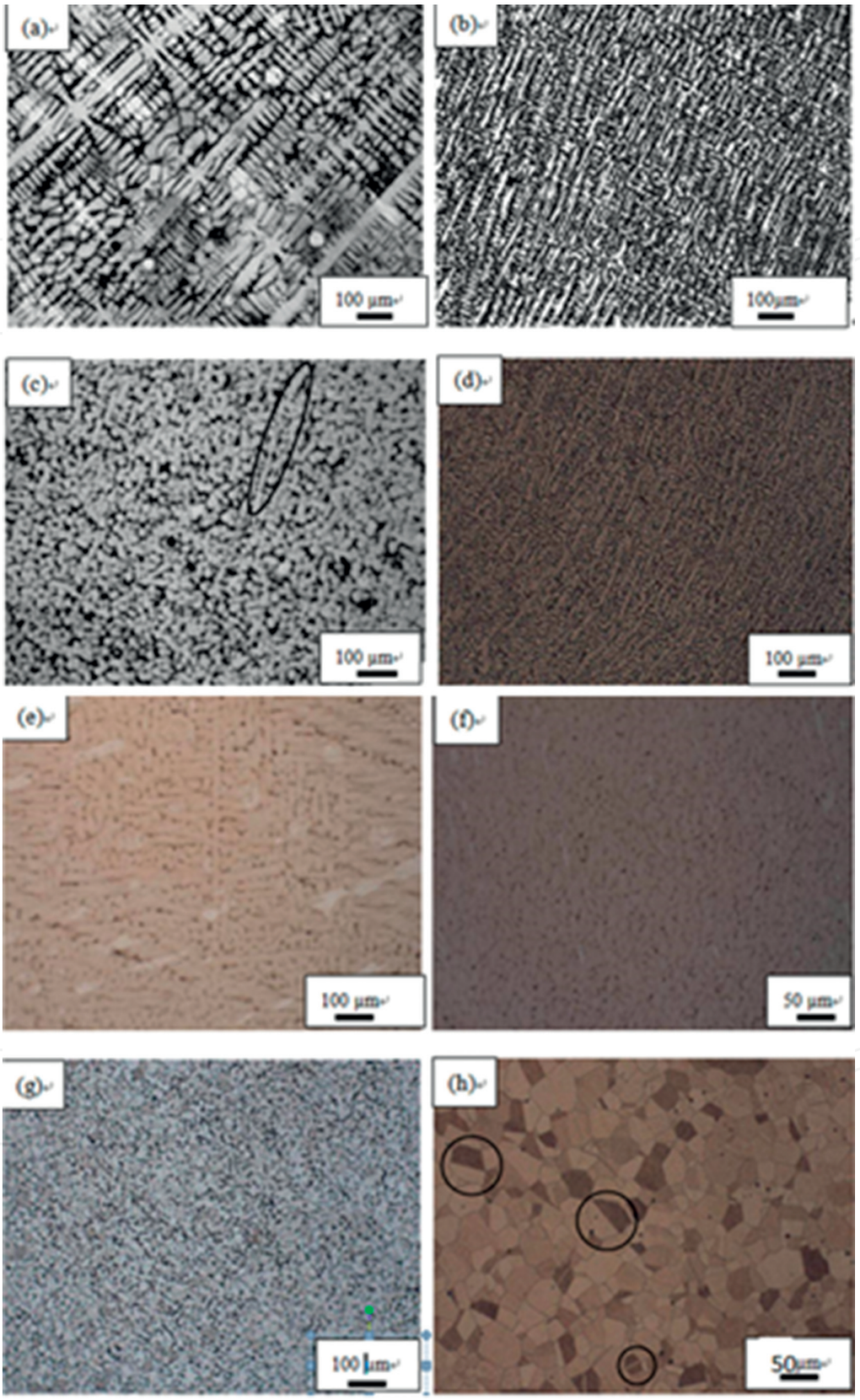

Figure 4. As-solidified microstructures of Ni-20at.%Cu alloy at small undercoolings: (a) ΔT = 17 K; (b) ΔT = 30 K; (c) ΔT = 72 K; (d) ΔT = 107 K; (e) ΔT = 158 K; (f) ΔT = 170 K; (g) ΔT = 182 K; (h) ΔT = 261 K.

growth has transformed from solute diffusion to thermal diffusion in the melt ahead of the dendrite tip. Here, ΔT_3 is defined as the characteristic undercooling at which there are no obvious dendrite fragments in the microstructures, and only large dendritic crystals are found (**Figure 4d** and **e**). At undercoolings larger than the critical value ΔT^* = 170 K, the overall microstructures are refined again (**Figure 4f** and **g**). As ΔT exceeds 182 K, the microstructures consist of completely fine equiaxed grains and there are many twins in the grains, see the black circles in **Figure 4h**. The formation of annealing twins in fcc metals and alloys are due to the growth accidents on {1 1 1} propagating steps present on migrating grain boundaries. As a result of the accidents, Shockley partial dislocations are generated contiguously to boundaries. These partial dislocations repel each other and glide away from the boundary to produce a twin.

When an alloy melt solidifies at a small undercooling, e.g., ΔT = 50 K in the case of undercooled Co-20%at.Pd, the advancement of solid/liquid (S/L) interface is controlled by solute diffusion ahead of the S/L interface. Solidification of the melt proceeds rather slowly and results in the formation of well-developed dendritic microstructures (see **Figure 5a**). With increasing undercooling, a grain refinement event is observed in the undercooled Co-20%at.Pd alloy at 50–265 K. The first grain refinement in an undercooled single phase alloy is generally believed to be caused by the remelting effect during the post-recalescence period. When ΔT reaches the range of 265–280 K, which is above the hypercooling limit, due to a zero remelting effect, the dendrite trunks cannot be remelted and therefore can be preserved in the solidification microstructure, leading to the presence of the elongated grained structure. The appearance of elongated grained structure in the hypercooled Co-20%at.Pd alloy is apparently ascribed to the vanished remelting effect in the post-recalescence period. As ΔT is higher than 280 K, the second grain refinement event occurs. The equiaxed grains with rather straight grain boundaries (see **Figure 5e** and **f**) strongly suggest that the formation of the solidification microstructure is due to recrystallization. The recrystallized microstructures in hypercooled alloys have been observed by Willnecker et al. in Co-20%at.Pd alloy and by Lu et al. in Ni75Pd25 alloy [12, 14]. In the present work, the occurrence of recrystallization in the hypercooled Co-20%at.Pd alloy with ΔT = 280 K was considered to be induced by the accumulation of internal strain/stress caused by the dramatic shrinkage stress resulting from rapid solidification. For rapid solidification taking place at a rather high undercooling, the advance of the solid/liquid interface proceeds extremely fast. As a consequence, a large volume contraction owing to rapid solidification will cause a high shrinkage stress developing in the system.

Three typical temperature profiles corresponding to the solidification of Co-20%at.Pd alloy melts in different undercooling regimes are shown in **Figure 6**. It was found that when ΔT = 265 K, the post-recalescence period presents in the temperature profiles, as seen in the plateau marked by the plateau duration time (Δt_{pl}) in **Figure 3a**. The plateau duration time Δt_{pl} is the time required for the residual liquid to transform into solid after recalescence. Δt_{pl} can be obtained by subtracting the time point of recalescence from the time point at which the first derivative of cooling curve after recalescence abruptly changes. When ΔT reaches 265 K, the

http://dx.doi.org/10.5772/intechopen.70666

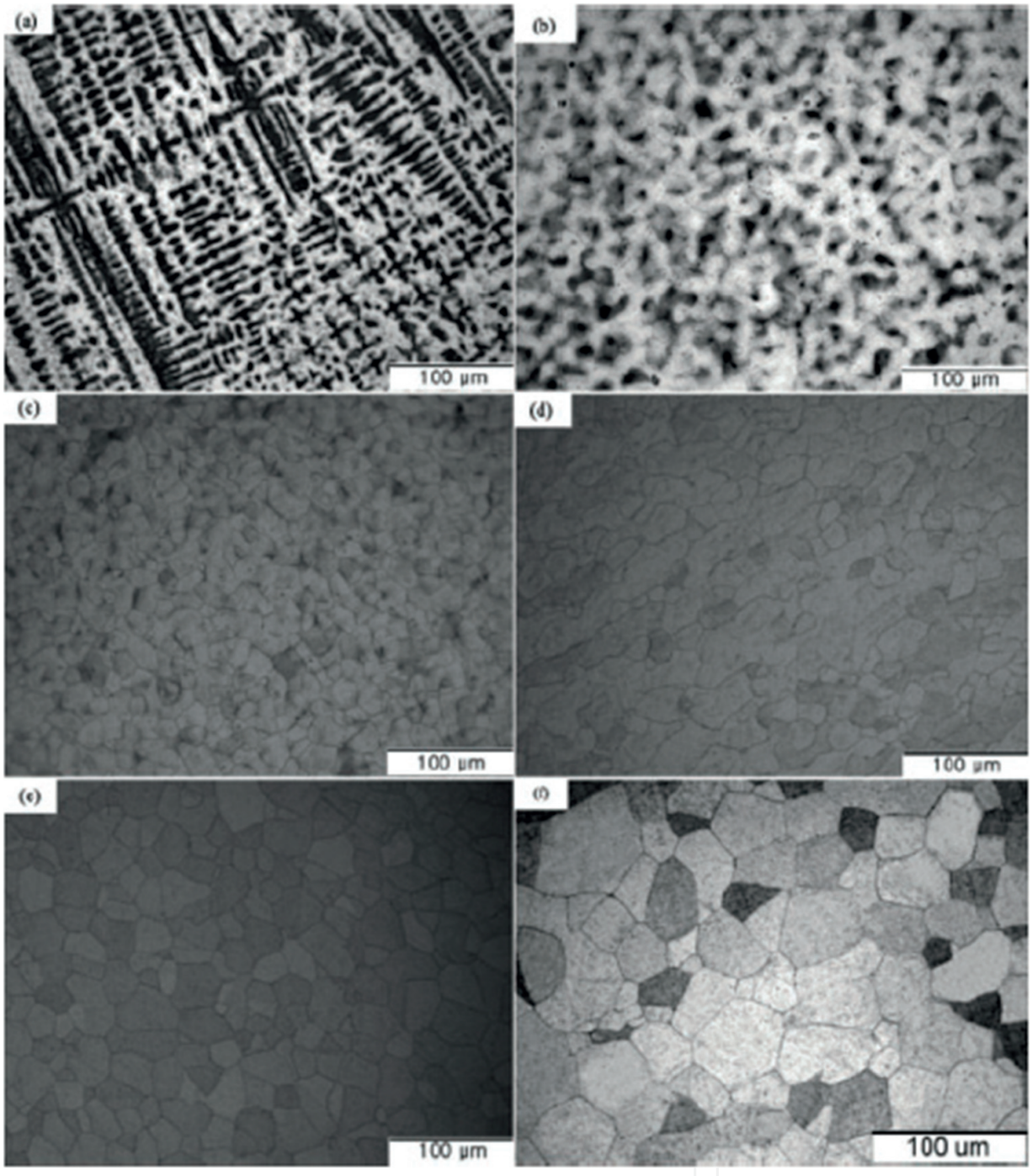

Figure 5. As-solidified microstructures of Co-20at.%Pd alloys undercooled by (a) 20 K, (b) 85 K, (c) 160 K, (d) 265 K, (e) 290 K, and (f) 340 K.

post-recalescence period does not appear, and the maximum recalescence temperature is lower than the solidus temperature of this alloy (see **Figure 3b** and **c**). Since the post-recalescence period will only vanish when the hypercooling limit of a metal is reached, the hypercooling limit of the Co-20%at.Pd alloy can be determined as 265 K.

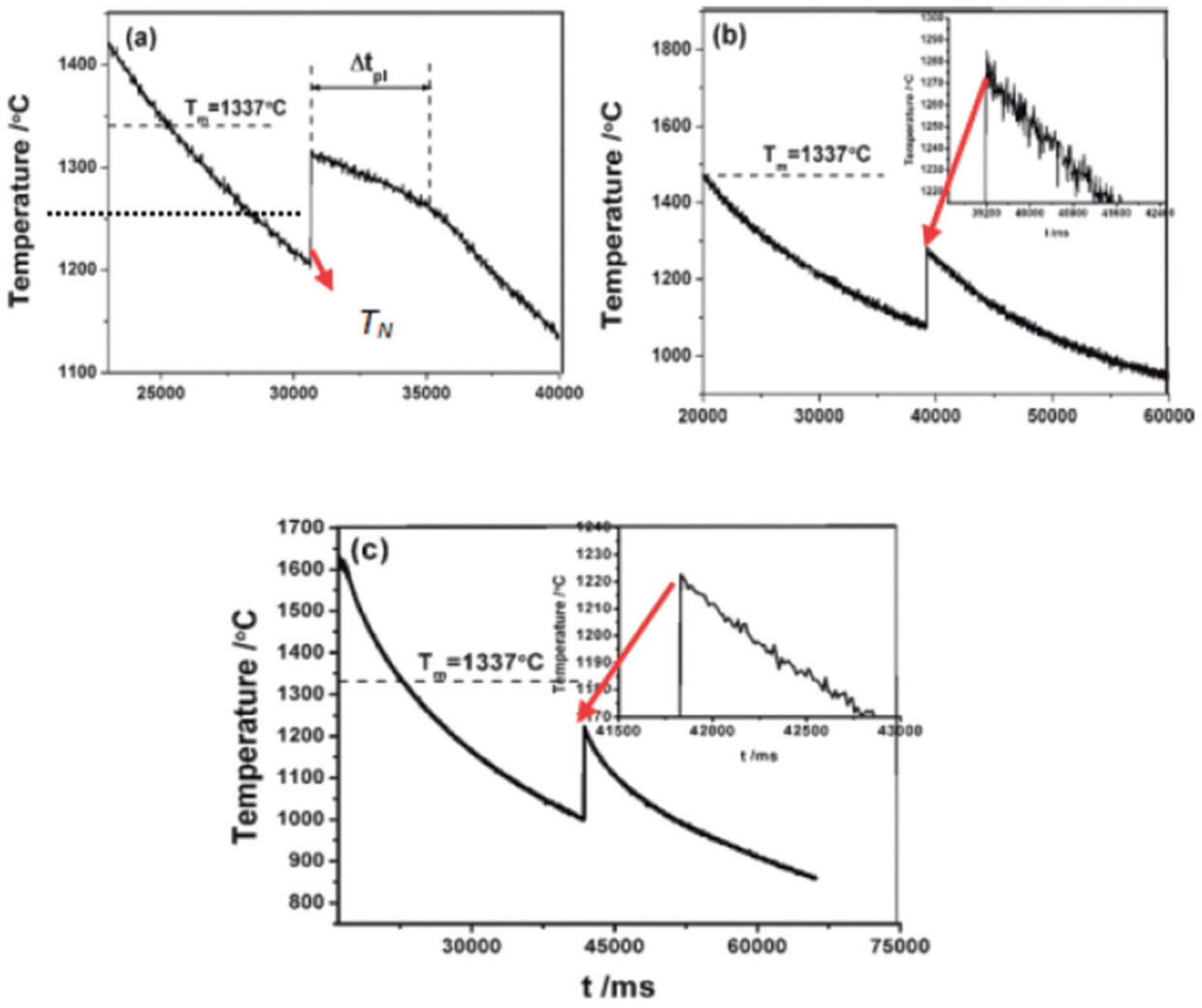

Figure 6. The measured average grain size as a function of initial undercooling of (a) Ni-20at.%Cu and (b) Co-20at.%Pd alloys.

6. Grain refinement mechanism of first refinement

The equilibrium phase diagram shows that the molten fraction of a solid alloy that has been heated into the solid-liquid binary phase regime is related to the chemical superheating [9]. Here, due to the non-equilibrium effect involved in rapid solidification of undercooled melts, it is reasonable to speculate that the non-equilibrium kinetic phase diagram can deal with the remelted fraction of the solid phase more realistically and practically. Then, extension of Li's model [9] will give a non-equilibrium chemical superheating model that can predict the remelted dendrite fraction by the following equation:

$$f_L = \frac{k(T_R - T_S)/\Delta T_0}{1 - (1-k)(T_R - T_S)/\Delta T_0} \tag{2}$$

This model is similar to Li's model [9], however it is an extended chemical superheating model considering the relaxation effect in undercooled liquid phase. In this extended model, k is the

non-equilibrium solute partition coefficient. T_R is the maximum recalescence temperature corresponding to initial undercooling ΔT, T_S is the non-equilibrium solidus temperature corresponding to the composition C_S of the central part in the dendrite stem, and ΔT_0 is the non-equilibrium crystallization temperature range of the alloy with composition C_S. The value of f_L shows the extent of the remelting induced breakup of the dendrites, so f_L can be used to evaluate the tendency of remelting.

The remelted fraction of the primary dendrite is shown in **Figure 4**. The obvious difference between Li's model and the present model is that the present model incorporates local non-equilibrium effect (i.e., the relaxation effect in the undercooled bulk liquid phase) in the model derivation. Thus, it can be further inferred that the remelted fraction of the primary dendrite of the present model is mainly influenced by the composition of liquid phase of the present model, in which the relaxation effect plays an important role [19]. In the present experiments, the first kind of grain refinement of rapidly solidified Ni-20%at.Cu alloy emerged in the undercooling range of about 40 K (ΔT_2) to 90 K (ΔT_3). In consistency with the prediction of the present extended chemical superheating model, the first kind of grain refinement found in the experiments lies in the undercooling range which has very strong remelting tendency of dendrites (**Figure 7**). Comparing the predicted results of the Li's model (local equilibrium condition) and the present model (local non-equilibrium condition), we can see that under low undercooling ranges, these two model predict similar results. Both model (**Figure 7**)

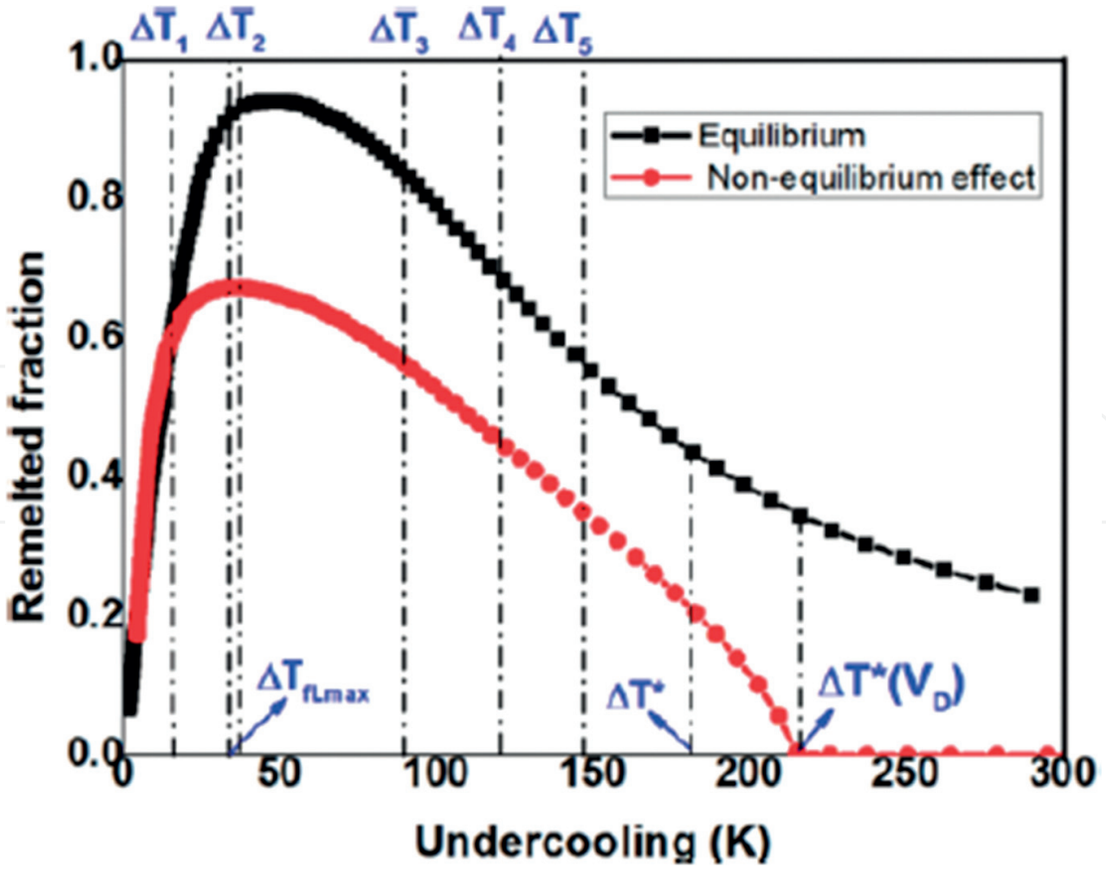

Figure 7. Remelted fraction of the primary dendrite at the highest recalescence temperature point in highly undercooled Ni-20at.%Cu.

predicts that the undercooling range of about 40–90 K has a strong dendrite remelting tendency, thus in this range the dendrites universally break up due to chemical superheating effect. While at high undercooling range severe discrepancy happens between these two models. As can be seen from **Figure 7** that, when the undercooling exceeds the critical undercooling ΔT^*, the discrepancy becomes more and more severe and achieves a maximum value at the undercooling value $\Delta T^*(V_D)$, i.e., the undercooling where the dendrite growth velocity exceeds the solute diffusion speed V_D in the undercooled liquid phase. Besides, at the undercooling value $\Delta T^*(V_D)$, the remelted fraction reaches zero and no chemical superheating induced dendrite remelting will happen. Thus, as previous study [10–18] showing, the grain refinement above the second critical undercooling ΔT^* is induced by the mechanisms of stress-induced breakup and recrystallization of the rapidly solidified dendrites, rather than dendrite remelting induced by chemical superheating, which can hardly affect the dendrite breakup in the high undercooling range as shown in **Figure 7**. Obviously, the significance of the present extended chemical superheating model is that it can predict good results in consistency with the experiment observation and the relaxation effect on non-equilibrium solidification of undercooled melt is clearly illustrated. The first grain refinement mechanism is also the chemical superheating mechanism and will not be given here for short. It has been revealed that the stress induced dendrite breakup and recrystallization process mainly occur during and after recalescence period. These two physical processes should be responsible for the grain refinement at high undercooling regimes [9].

7. Stress induced recrystallization mechanism ($\Delta T > \Delta T^*$)

Many researches [7–9, 15–17] have revealed that the stress induced recrystallization process mainly during recalescence period should be responsible for the grain refinement at high undercooling range. However, few strong and direct evidences have been found to support this speculation. We also have revealed this phenomenon in hypercooled Co-20at.%Pd alloys and found strong and direct evidences, see Ref. [13].

When the fraction of the solid phase exceeds about 10% during recalescence, the coherent dendrite networks are usually established [7, 9]. During rapid recalescence, as the dendrite fraction increases, the inter-dendritic permeability correspondingly decreases [7, 9]. Consequently the pressure gradient in the first mushy zone (FMZ) increases. The pressure gradient induces the inter-dendritic flow of liquid phase and therefore stress accumulated in the solid phase in the FMZ [9]. Considering inter-dendritic flow of melt induced by both solidification contraction and thermal strain, we will build a corrected stress accumulation model for rapid solidification of an undercooled melt was established. According to Ref. [9], the liquid volume flux $U(x)$ among dendrites can be expressed as:

$$U\left(\vec{x}\right) = \frac{\left|\vec{a}\right|}{t_f}\left[\beta_s\left(f_R^s - f_s\left(\vec{x}\right)\right)\right] \tag{3}$$

where $\vec{a}$ is the size of FMZ in which primary growth or recalescence occurs, t_f is the total solidification time of the primary phase, i.e., the recalescence time, $\beta_s=(\rho_l-\rho_s)/\rho_s$ is the

solidification shrinkage of the primary phase, ρ_l and ρ_s are densities of liquid and solid phases respectively. f_R^s is the fraction of solid at the maximum recalescence temperature, f_s is the solid fraction during recalescence and $\vec{x}$ is the local position in the One-dimensional space coordinates.

The thermal strain induced inter-dendritic flow of liquid phase $U^{'}(\vec{x})$ in the mushy zone can be expressed as [22]:

$$U^{'}\left(\vec{x}\right) = -(1+\beta_s)\dot{E}\left(\vec{x}\right) \tag{4}$$

where $\dot{E}(x)$ is the accumulated strain rate in the dendrites and can be defined as [16]:

$$\dot{E}\left(\vec{x}\right) = \int f_s \dot{\varepsilon}\left(\vec{x}\right) d\,\vec{x} \tag{5}$$

where $\dot{\varepsilon}(\vec{x}) = \nabla v_{\vec{x}}(\vec{x})$ is the strain rate in the dendrites and $\dot{\varepsilon}(\vec{a}) = 0$.

According to Eq. (6) in Ref. [7] and Eq. (4), the total volume flow of molten feeding liquid is:

$$U_{total}\left(\vec{x}\right) = \frac{\left|\vec{a}\right|}{t_f}\left[\beta_s\left(f_R^s - f_s\left(\vec{x}\right)\right)\right] + (1+\beta_s)\int f_s\left(\vec{x}\right)\dot{\varepsilon}\left(\vec{x}\right) d\,\vec{x} \tag{6}$$

According to Darcy's equation, as demonstrated in Ref. [22], the pressure gradient in the liquid phase can be expressed as [16]:

$$-\nabla P_l\left(\vec{x}\right) = \frac{\mu}{K} U_{total}\left(\vec{x}\right) \tag{7}$$

where P_l is the pressure in the liquid phase during solidification, μ the dynamic viscosity and K the permeability of the two phase region as demonstrated in Ref. 17. According to the Carman-Kozeny relation demonstrated in Ref. 17, K can be expressed as [16]:

$$K = \frac{1}{5S_V^{s-l}\left(\vec{x}\right)^2}\frac{f_l\left(\vec{x}\right)^3}{f_s\left(\vec{x}\right)^2} = \frac{\lambda_2^2\left(\vec{x}\right)}{80}\frac{f_l\left(\vec{x}\right)^3}{f_s\left(\vec{x}\right)} \tag{8}$$

where $G_L(\vec{x})$ is the temperature gradient ahead of the liquid/solid interface. $S_V^{s-l}(\vec{x})$ is.

the area of the dendrites in unit volume and $S_V^{s-l}(\vec{x}) = 4/\left(\sqrt{f_s(\vec{x})}\lambda_2(\vec{x})\right)$, $\lambda_2(\vec{x})$ is the spacing between secondary dendrite arms [23]. Applying linear micro-segregation model, as demonstrated in Ref. [23]:

$$dT/df_l\left(\vec{x}\right) = \Delta T_0 \tag{9}$$

where ΔT_0 is the solidification interval of the alloy. Using Eqs. (7)–(9) in combination with Eq. (12) in Ref. [7], the pressure of the mushy zone can be expressed as:

$$P\left(\vec{x}\right)=P_0-\frac{160\mu\cdot\left|\vec{a}\right|^2\cdot\beta_s}{\left(f_R^s\right)^2 t_f\lambda_2^2}\left[f_s\left(\vec{x}\right)-f_{coh}\left(\vec{x}\right)+\frac{1}{1-f_s\left(\vec{x}\right)}-\frac{1}{1-f_{coh}\left(\vec{x}\right)}+2\ln\frac{1-f_s\left(\vec{x}\right)}{1-f_{coh}\left(\vec{x}\right)}\right]$$
$$+\left\{\frac{320\left(1+\beta_s\right)\cdot\mu\cdot\left|\vec{a}\right|\cdot\Delta T_0\cdot\dot{\varepsilon}}{3G_S\cdot\left(f_R^s\right)^2\cdot\lambda_2^2}\int_{f_{coh}}^{f_s}\frac{f_s\left(\vec{x}\right)}{f_l\left(\vec{x}\right)^3}\left[f_s\left(\vec{x}\right)^3-f_{coh}\left(\vec{x}\right)^3\right]df_s\left(\vec{x}\right)\right\} \tag{10}$$

where f_{coh} is the fraction solid at the dendrite coherency point. The second term in Eq. (10) considers the liquid flow induced by thermal strain during rapid solidification. We can describe the thermal strain as:

$$\varepsilon=\alpha_{ther}(T-T_s) \tag{11}$$

where α_{ther} is a coefficient of thermal expansion. T_s is solidus temperature. Differentiating Eq. (10), we obtain thermal strain rate:

$$\dot{\varepsilon}=\alpha_{ther}\dot{T} \tag{12}$$

We define average thermal strain as:

$$\overline{\dot{\varepsilon}}=\alpha_{ther}\frac{\Delta T}{\Delta t} \tag{13}$$

In order to estimate the accumulated stress in the dendrites, we consider the one dimensional case. Then the momentum equation in solid phase is, as demonstrated in Ref. [24]:

$$0=\nabla\left[f_s\left(\vec{x}\right)\sigma_s\left(\vec{x}\right)\right]+M_s^{\tau}\left(\vec{x}\right) \tag{14}$$

where $\sigma_s(\vec{x})$ is the x component of the stress in the solid phase and M_s^{τ} is the interfacial stress due to interaction with the liquid phase. The interfacial stress exerted upon the solid network from flowing liquid phase can be given as, as demonstrated in Ref. [24]:

$$M_s^{\tau}\left(\vec{x}\right)=P_l\left(\vec{x}\right)\nabla f_s\left(\vec{x}\right)+M_s^d\left(\vec{x}\right) \tag{15}$$

where $M_s^d(\vec{x})$ is the dissipation of stress of interface and can be expressed by Darcy Eq., as demonstrated in Ref. [24]:

$$M_s^d\left(\vec{x}\right)=\frac{f_l\left(\vec{x}\right)\mu}{K}U_{total}\left(\vec{x}\right)=-f_l\left(\vec{x}\right)\nabla P_l\left(\vec{x}\right) \tag{16}$$

In combination with Eq. (16), the stress in the dendrite coherency obeys the following equation [24]:

$$-\nabla\left[f_s\left(\vec{x}\right)\sigma_s\left(\vec{x}\right)\right] = P_l\left(\vec{x}\right)\nabla f_s\left(\vec{x}\right) - f_l\left(\vec{x}\right)\nabla P_l\left(\vec{x}\right) = -\nabla\left[P_l\left(\vec{x}\right)f_l\left(\vec{x}\right)\right] \tag{17}$$

At the start of the coherent part of the first mushy zone, which is abbreviated as FMZ, the solid stress is equal to the hydrostatic pressure, i.e., $\sigma_s = -P_0$, where P_0 is the pressure in the liquid phase when the mushy zone starts to form. $f_s(\vec{x})$ is the solid fraction of the dendrite coherency. Integrating Eq. (10), we can obtain:

$$\sigma_s\left[f_s\left(\vec{x}\right)\right] = \frac{1}{f_s\left(\vec{x}\right)}\left[-P_0 + P_l\left(\vec{x}\right)f_l\left(\vec{x}\right)\right] = -\left[P_0 + \frac{f_l\left(\vec{x}\right)}{f_s\left(\vec{x}\right)}\Delta P_l\left(\vec{x}\right)\right] \tag{18}$$

where $\Delta P_l = P_0 - P_l$ is the pressure drop in the liquid phase. Using Eqs. (10), (13) and (18), the stress resulted from inter-dendritic liquid flow induced by both solidification shrinkage and thermal strain is:

$$\sigma_s = \frac{160\mu\cdot\left|\vec{a}\right|}{\left(f_R^s\right)^2 t_f \lambda_2^2} \times \frac{\left(1 - f_s\left(\vec{x}\right)\right)}{f_s\left(\vec{x}\right)} \left\{ \left|\vec{a}\right|\cdot\beta_s \left[\begin{array}{l} f_s\left(\vec{x}\right) - f_{coh} + \dfrac{1}{\left(1 - f_s\right)} - \dfrac{1}{\left(1 - f_{coh}\right)} \\ +2\ln\left[\dfrac{1 - f_s\left(\vec{x}\right)}{1 - f_{coh}}\right] \end{array} \right] \right.$$

$$\left. - \frac{2\left(1 + \beta_s\right)\alpha_{ther}\Delta T_0 \Delta T}{3G_S} Q\left[f_s\left(\vec{x}\right)\right] \right\} \tag{19}$$

where

$$Q\left[f_s\left(\vec{x}\right)\right] = \int_{f_{coh}}^{f_s} \frac{f_s\left(\vec{x}\right)}{f_l\left(\vec{x}\right)^3}\left[f_s\left(\vec{x}\right)^3 - f_{coh}\left(\vec{x}\right)^3\right] df_s\left(\vec{x}\right) \tag{20}$$

Considering inter-dendritic flow of liquid induced by both solidification contraction and thermal strain, an analytic model of stress accumulation during rapid solidification of undercooled melts was established in the present work. According to this model, the stress accumulated in the dendrite coherency can be calculated by Eq. (19). G_S is temperature gradient of solid phase, respectively. In the current work, it is assumed that $\lambda_2 = \alpha R_{tip}$. Using the physical parameters listed in **Table 1**, σ_s as a function of ΔT can be calculated by Eqs. (19) and (20), as shown in **Figure 8**.

It can be seen from **Figure 8** that, with increasing ΔT, σ_s continuously increases. Once σ_s exceeds the yielding strength of the alloys, the dendrite networks will be plastically deformed, leading to dense dislocations and annealing twins and a storage of micro-strain in the

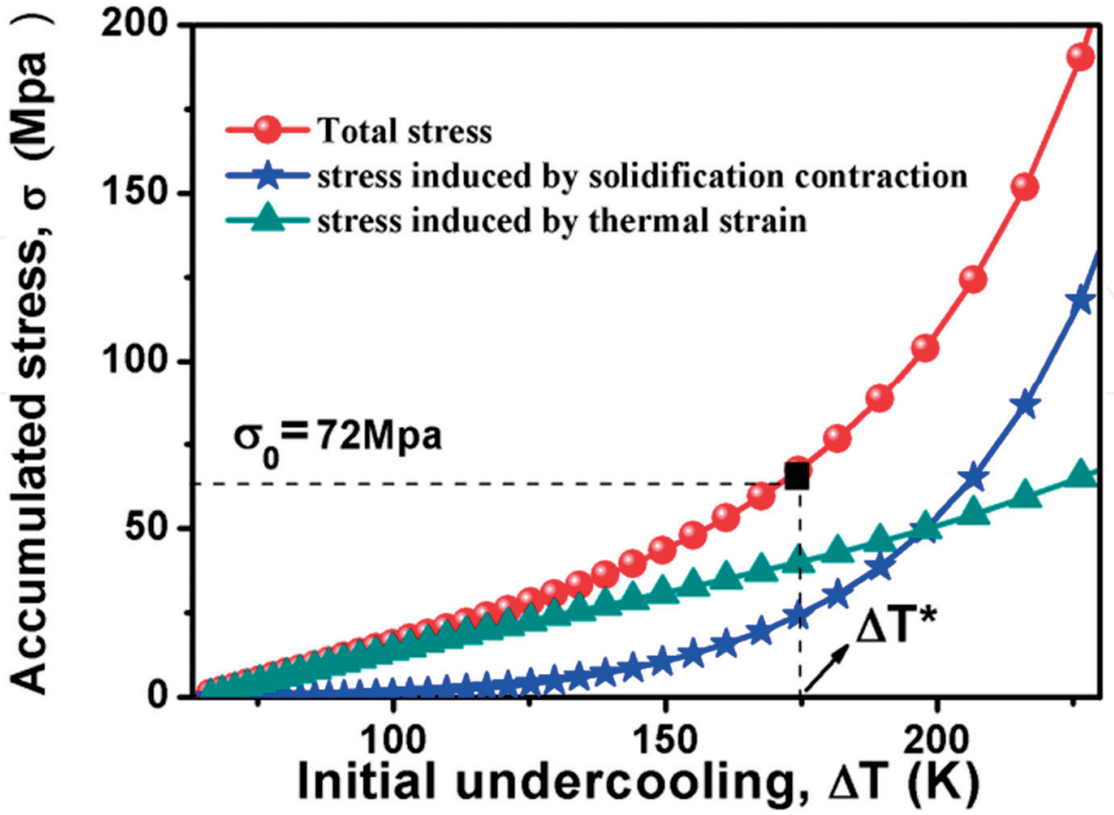

Figure 8. Calculated stress accumulated in dendrite skeleton during rapid solidification of Ni-20at.%Cu alloys as a function of initial undercoolings: the dashed line represents yielding strength the alloys.

microstructures. **Figure 9a–c** show the dense dislocation networks in the grain of Ni-20at.%Cu alloy. The white circle in **Figure 9d** shows an annealing twin in the microstructure. **Figure 8e** shows the electron diffraction spots of the annealing twin in **Figure 9d**. The electron diffraction spots are typical diffraction spot of twins in a FCC alloy. As is known, the stored micro-strain will act as the driving force for recrystallization. Further increasing ΔT causes a continuous increase of the stored micro-strain, resulting in a continuous increase in the extent of deformation. Once the stored energy due to deformation is high enough to initiate the nucleation, the recrystallization will take place. Consequently, a refined recrystallized microstructure can be produced.

Generally, recrystallization is a physical process and consists of two basic processes: the site saturation nucleation which proceeds by atomic thermal activation and the growth of the new strain free grains, when being annealed at temperatures above a proper recrystallization temperature, which is the atomic thermal activation temperature. In order to reveal the recrystallization process in the rapid solidification microstructures of the Ni-20at.%Cu alloys, recrystallization annealing experiments were performed for the quenched and naturally cooled alloys, see in the reference [14]. Compared to the naturally cooled alloys which did not undergo recrystallization. However, as a comparison, the recrystallization drives the microstructures of the quenched alloys to transform into completely newly formed microstructures.

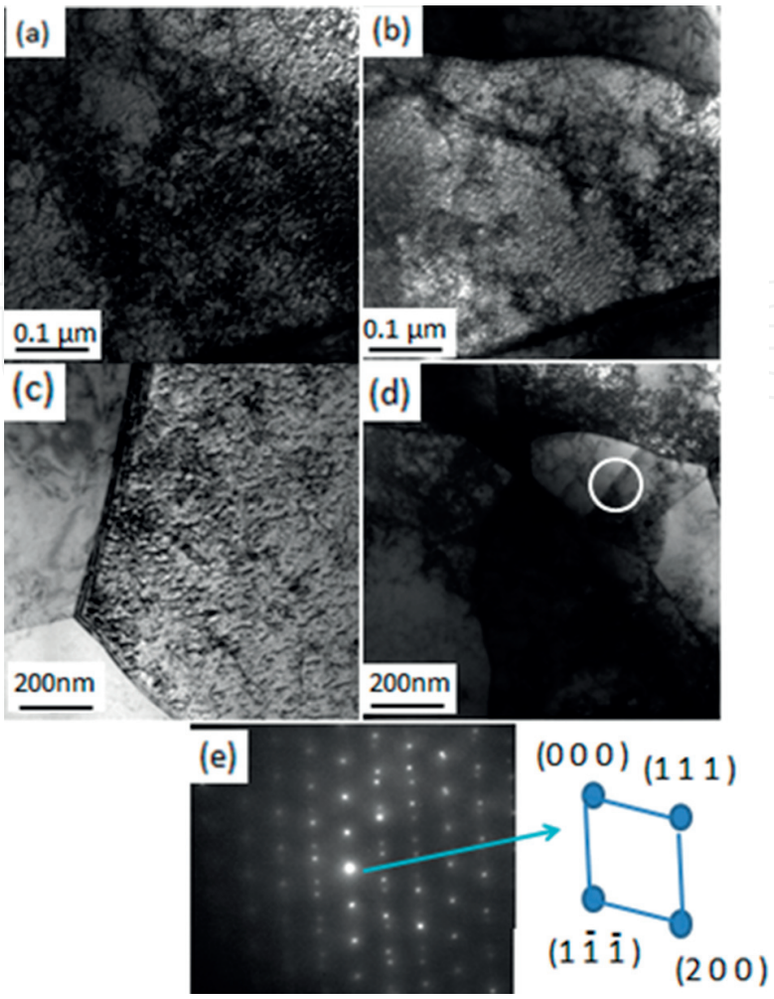

Figure 9. TEM bright field image of (a–d) the dense dislocations and (e) annealing twins in the rapidly solidified $Ni_{80}Cu_{20}$ alloy quenched with a undercooling of about 220 K (220°C).

8. Conclusions

Applying molten glass purification method combined with cyclic superheating method, non-equilibrium microstructural evolution and grain refinement mechanisms of Ni-20at.% Cu and Co-20at.%Pd alloy were investigated systematically. The main conclusions are as follows:

1. Ni-20at.%Cu and Co-20at.%Pd alloy were undercooled by means of fluxing method. Two grain refinement events of the solidification microstructures were observed. The first grain refinement was attributed to chemical superheating induced dendrite remelting. The second grain refinement was ascribed to stress induced recrystallization of the rapidly solidified dendrites.

2. The relationship between the dimensionless superheating and the undercooling indicates that the grain refinement occurring at low undercoolings results from the dendrite break-up

owing to the dendrite remelting, but at high undercooling the dendrite remelting effect is weak.

3. With the help of incorporating the relaxation effect of solute diffusion in bulk undercooled liquid, an extended chemical superheating model for predicting dendrite remelting was developed to explain the two kinds of grain refinement events occurring in the low and high undercooling regimes respectively. It was found that the present dendrite remelting model could predict relatively good results in consistency with the grain refinement event observed in the experiments.

4. It can be inferred that the rapid dendrite growth, the dendrite deformation and the stress-induced dendrite break-up occur during recalescence stage; the solidification of the residual liquid phase, the remelting of dendrites, the recrystallization and the grain growth (secondary recrystallization) occur during post-recalescence period.

5. A corrected model was developed to semiquantitatively calculate the stress accumulation during rapid solidification of undercooled Ni-20at.%Cu alloys. When the undercooling is larger than a critical value, the stress due to solidification contraction and thermal strain will cause break-up of the primary dendrites. The strain energy stored in the broken dendrite pieces will drive recrystallization, leading to a grain refined recrystallization microstructures

Acknowledgements

The authors are grateful to the financial support of National Basic Research Program of China (973Program, 2011CB610403). This work is also supported by International Cooperation Project Supported by Ministry of Science and Technology of China (No. 2011DFA50520).

Conflicts of interest

The authors have no conflicts of interest

Author details

Xiaolong Xu[1,2]*, Hua Hou[1] and Feng Liu[2]

*Address all correspondence to: xiaolong@nuc.edu.cn

1 College of Materials Science and Engineering, North University of China, Taiyuan, Shanxi, People's Republic of China

2 State Key Laboratory of Solidification Processing, Northwestern Polytechnical University, Xi'an, Shaanxi, People's Republic of China

References

[1] Walker JL. The Physical Chemistry of Process Metallurgy, Part 2. New York: Interscience; 1959

[2] Baker JC, Cahn JW. Solidification. 1st ed. Metals Park, OH: ASM; 1971

[3] Dragnevski K, Cochrane RF, Mullis AM. Splitting in deeply undercooled, ultrahigh purity Cu.Physical Review Letters. 2002;**89**:215502

[4] Mullis AM, Cochrane RF. Dendrites Grain refinement and the stability of dendrites growing into undercooled pure metals and alloys. Journal of Applied Physics. 1997;**82**:3783

[5] Powell GLF. Comments on "Undercoolability of copper bulk samples". Journal of Materials Science Letters. 1991;**10**:745

[6] Herlach DM. Materials Science and Engineering R. 1994;**R12**:177-272

[7] Liu F, Yang GC. Stress-induced recrystallization mechanism for grain refinement in highly undercooled superalloy. Journal of Crystal Growth. 2001;**231**:295-305

[8] Karma A. Model of grain refinement in solidfication of undercooled melts. International Journal of Non-Equilibrium Processing. 1998;**11**:201

[9] Li JF, Liu YC, Lu YL, Yang GC, Zhou YH. Structural evolution of undercooled Ni–Cu alloys. Journal of Crystal Growth. 1998;**192**:462-470

[10] Christian JW. The Theory of Transformation in Metals and Alloys. Oxford: Pergamon Press; 2002. p. 832-858

[11] Piccone TJ, Wu Y, Shiohara Y, Flemings MC. Dendritic Growth of Undercooled Nickel-Tin: Part III. Metallurgical Transactions A. 1987;**18A**:925-932

[12] Lu SY, Li JF, Zhou YH. Grain refinement in the solidification of undercooled Ni–Pd alloys. Journal of Crystal Growth. 2007;**309**:103-111

[13] Xu XL, Chen YZ, Liu F. Evidence of recrystallization mechanism of grain refinement in hypercooled Co 80 Pd 20 alloys. Materials Letters. 2012;**81**:73-75

[14] Lu SY, Li JF, Zhou YH. Recrystallization developed in the largely undercooled Ni 54.6 Pd 45.4 alloy. Journal of Alloys and Compounds. 2008;**458**:517-522

[15] Wilde G, Gorler GP, Willnecker R. Specific Heat Capacity of Undercooled Magnetic Melts. Applied Physics Letters. 1996;**69**:2995-2997

[16] Dahle AK, Thevik HJ, Arnberg L, John DH. St. Metallurgical and Materials Transactions B. 1999;**30**:287

[17] Humphreys FJ, Hatherly M. Recrystallization and Related Annealing Phenomena. 2nd ed. New York: Oxford; 2004

[18] Xu XL, Liu F. Observation of recrystallization upon annealing rapidly solidified microstructures of highly undercooled Ni 80 Cu 20 alloys. 2014;**597**:205-210

[19] Galenko PK, Danilov DA. Physics Letters A. Local nonequilibrium effect on rapid dendritic growth in a binary alloy melt. 1997;**235**:271-280

[20] Xu XL, Hou H, Liu F. Nonequilibrium Solidification, Grain Refinements, and Recrystallization of Deeply Undercooled Ni-20 At. Pct Cu Alloys: Effects of Remelting and Stress. Metallurgical and Materials Transactions A: Physical Metallurgy and Materials Science. 2017;1-9

[21] Bhattacharya A, Dutta P. Effect of shrinkage induced flow on binary alloy dendrite growth: An equivalent undercooling model. International Communications in Heat and Mass Transfer. 2014;**57**:216-220

[22] Bhattacharya A, Karagadde S, Dutta P. An equivalent undercooling model to account for flow effect on binary alloy dendrite growth rate. International Communications in Heat and Mass. Transfer. 2013;**47**:15

[23] Thevik HJ, Mo A. The influence of micro-scale solute diffusion and dendrite coarsening upon surface macrosegregation. International Journal of Heat and Mass Transfer. 1997; **40**:2055

[24] Ni J, Beckermann C. A volume-averaged two-phase model for transport phenomena during solidification. Metallurgical Transactions B. 1991;**22**:349